Distribution Categories:
Magnetic Fusion Energy (UC-20)
MFE--Magnetic Systems (UC-20b)
MFE--Fusion Systems (UC-20d)

ANL/FPP/TM-200

ANL/FPP/TM--200

DE85 010413

ARGONNE NATIONAL LABORATORY
9700 South Cass Avenue
Argonne, Illinois 60439

EFFECTS OF FORMVAR COATING AND COPPER-NICKEL OUTER SHEATH ON THE AC LOSSES OF MULTI-STRAND SUBSIZE CABLES

by

S. H. Kim

Fusion Power Program

February 1985

TABLE OF CONTENTS

LIST OF FIGURES

LIST OF TABLES

ABSTRACT

AC losses of two subcables, one with Formvar coating on the strands of the BNL 12-ml NbTi/Cu/CuNi conductor and another without the coating, were measured using the ANL Subcable Test Facility. The results indicate that couplings among the strands with and without the Formvar coating were quite weak. Weak coupling of the bare strands is due to the high resistance of the copper-nickel outer sheath. In the regime of $\dot{B} = 0 \sim 1.2$ T/s and $B = 0 \sim 4$ T, the magnetic diffusion time constant was $(3.8 - 5.7) \times 10^{-3}$ s.

1. INTRODUCTION

High current superconductors for toroidal and poloidal field coils of tokamaks may be subdivided to reduce ac losses under normal operations or default conditions of the machine. In a developmental stage coupling losses of the multistrands of a subsize conductor must be minimized by reducing the electrical contact among the strands. Formvar coating is one of the most commonly used forms of insulation for magnet wires. Since there is no systematic data for the durability of the Formvar coating under cyclic strain or under the friction among the strands at liquid helium temperatures, it is necessary to measure the worst case ac losses due to the coupling of the bare strands of a subcable. The purpose of this study is to determine the magnetic diffusion time constant of subcables from the measurements of the ac losses in pulsed fields. Two triplex subcables were fabricated for the ac loss measurements, one with Formvar coating on the strands of the BNL 12-mil conductor of NbTi/Cu/CuNi and another without the coating. AC losses of the two cables were measured using the ANL Subcable Test Facility, which is described in the following section.

2. SUBCABLE TEST FACILITY

2.1 G-10 Cryostat

To avoid excessive boiling of the liquid helium during the rapid charge and discharge of the coil, the cryostat is made using commercially available G-10 cylinders. The inner helium cylinder has an inner diameter of 31 cm, a depth of 170 cm, and a wall thickness of 0.31 cm. The outer cylinder has an inner diameter of 40 cm and a wall thickness of 0.62 cm. The bottom dome of the helium cylinder was fabricated by a wet lay-up method of fiberglass epoxy. The resin used for the assembly of the cryostat was Shell Epon 815 with General Mills Versamid 140 as curing agent in a volume ratio of one to one.

To reduce the radiation heating from the cryostat walls and bottom, superinsulation was wrapped on the outer surface of the helium cylinder. It consists of 30 layers of 6.35×10^{-3} mm-thick, double aluminized Mylar interweaved with Dexter paper. Helium loss due to the radiation heat with a helium level of 75 cm from the bottom was approximately 1.5 W. With instrumentation wires and two pairs of 1000-A current leads installed for the pulsing coil and testing sample coil, total helium losses in a stand-by condition were approximately 4.9 W.

2.2 Power Supplies

The pulsing power supply for the operation of the superconducting coil is an 80-kW rectifier. It has a pulsing current of triangular waveform and is rated for dc operation at 100 V and 800 A. Another power supply available for the pulsing coil is made up of four power supplies in one cabinet, each rated for dc operation at 100 V and 1250 A. Possible operating modes for the power supply are all in parallel with an output of 100 V, 5000 A, and all in series with an output of 400 V, 1250 A.

2.3 Pulsed Superconducting Coils

In order to provide a pulsing background field for testing conductors, two split-pair coils were fabricated. Some coil parameters are listed in Table 1. The conductor for coil A is a 19-strand subcable which is compacted but not soldered. The conductor structure is similar to the subcable

Table 1

Parameters of the Pulsed Coils

	Coil A	Coil B
Peak field, T	6.1 T at 640 A	6.2 T at 550 A
Inner diameter, mm	21	21
Outer diameter, mm	124	81
Axial length, mm	184	110
Number of turns	2176	1588
Conductor length, m	978	504
Inductance, mH	196	95
Coil current density, A/mm^2	147	132
Stored energy, kJ	40	14

for the ANL 3.3-MJ coil.[1] The conductor for coil B is a seven-strand subcable (six superconducting strands around one copper wire).

A typical pulsing mode for coil A is shown in Fig. 1. The unbalanced voltage, V_u, shows a few disturbances in the coil for pulsing with a peak current of 640 A as shown in Fig. 1(a). For pulsing with a peak current of 665 A as shown in Fig. 1(b), the unbalanced voltage indicates that some sections of the coil become normal and recover below a current level of 100 A. Quench or recovery of the coil depends on the pulsing period and $\dot{B}$ of the coil.

3. LOSS MEASUREMENTS

3.1 Superconductor

Parameters of the superconducting composite strand used for the measurements are listed in Table 2. The strand has the outer sheath of CuNi. Two kinds of triplex of 3 × (6 SC + 1 Cu) were fabricated as shown in Fig. 2, one with bare superconducting strand and another with Formvar insulation on the strand. The Formvar insulation was done by Essex of Fort Wayne, Indiana as a single pass of a standard commercial process.

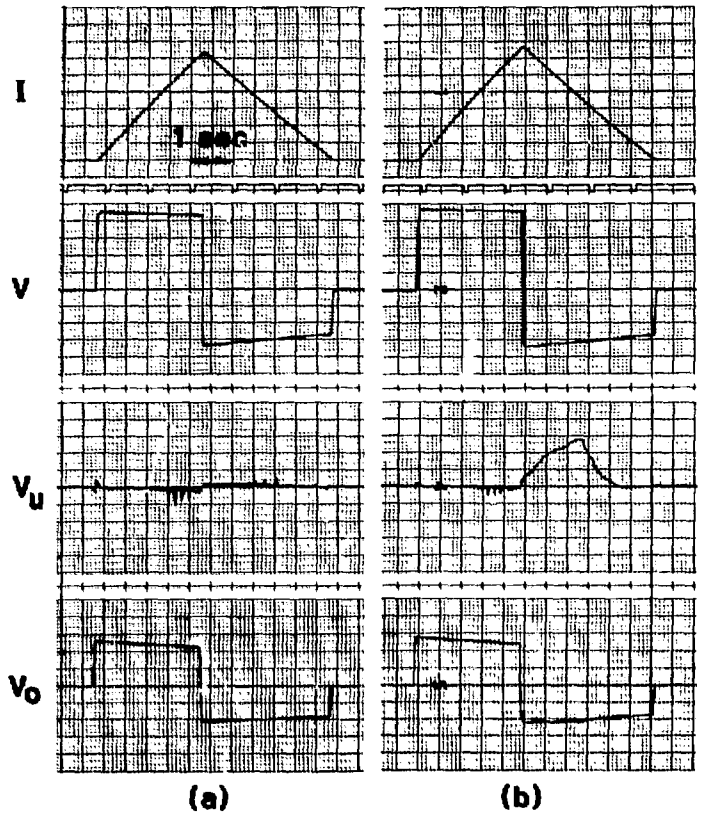

Fig. 1. Typical operating mode of the pulsed coil. I, pulsing current (20 A/div.); V, coil terminal voltage (2 V/div.); V_u, unbalanced voltage adjusted between V and V_o; V_o, voltage of one outer layer of a split coil (0.1 V/div.); and (a) peak curent of 640 A is less than the critical current; and (b) peak current of 665 A is above the critical current.

Table 2

Superconducting Composite Strand

Diameter, mm	0.305
(Cu + CuNi)/NbTi ratio	1.25
Filament diameter, μm	9
Number of filaments	510
Filament twist pitch length, mm	10

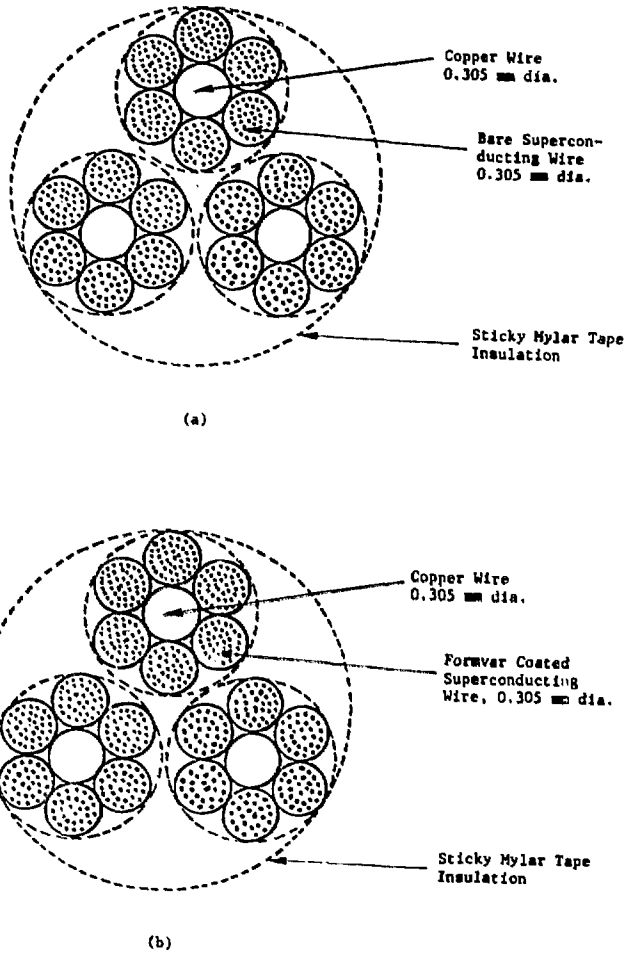

Fig. 2. Triplex cables: (a) without Formvar coating on the superconducting wire; and (b) with Formvar coating on the superconducting wire.

The triplex cables were fabricated by the New England Electric Wire Corp. of Lisbon, New Hampshire, according to ANL specifications. The six superconductors were twisted around one copper wire with a twist pitch length of 1.27 cm. The twist pitch length of the triplex cable is approximately 2.54 cm. During both stages of the cabling, the strands were not compacted. After the cabling, two layers of sticky Mylar tapes were wrapped as the turn-to-turn insulation of the sample coils.

3.2 Sample Coil and Helium Container

Sample coils of the two triplex cables were wound noninductively on G-10 bobbins. Parameters of the sample coils are listed in Table 3. The sample coil is located inside a separate G-10 helium container as shown in Fig. 3.

Table 3

Sample Coil Parameters

Inner diameter, mm	27
Outer diameter, mm	113
Axial length, mm	25
Number of turns	146
Cable length, m	32
Conductor volume, m^3	49.0×10^{-6}

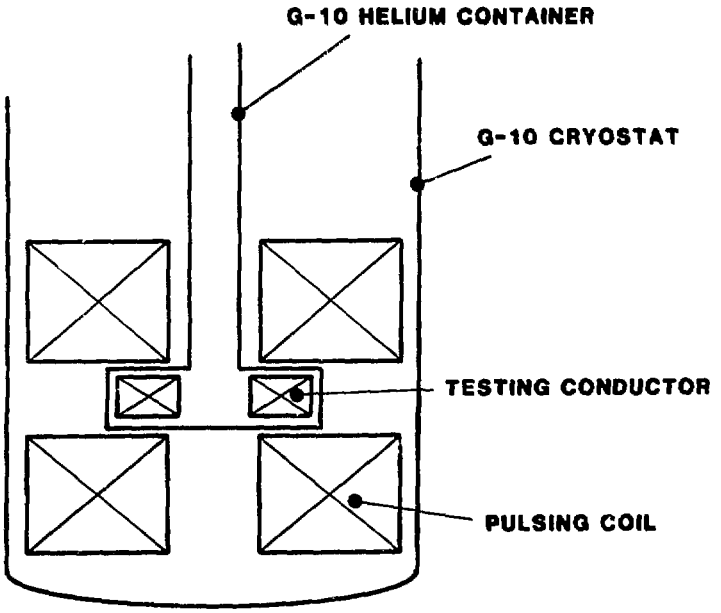

Fig. 3. Cross-sectional view of the helium container inserted between the split coil (diameter = 13 cm, G-10 cylinder height = 50 cm).

A G-10 cylinder (length = 60 cm, inner diameter = 2.2 cm) is attached to the helium container. The helium boil-off and a helium level change of 1 cm

inside the cylinder is equivalent to approximately 10.7 J of heat generation. Liquid helium was transferred to the G-10 containter by overflowing the helium from the G-10 cryostat to the inside of the cylinder. Possible liquid helium leaks of the helium container were tested for more than two hours when the helium level of the G-10 cryostat was about 30 cm lower than that of the cylinder.

3.3 Experimental Data and Discussions

Figure 4 is a typical pulsing mode during the measurements of the helium boil-off from the sample coil in the G-10 helium container. Charging and discharging times for the pulsing coil are in the range of 2.5 to 4.5 s with

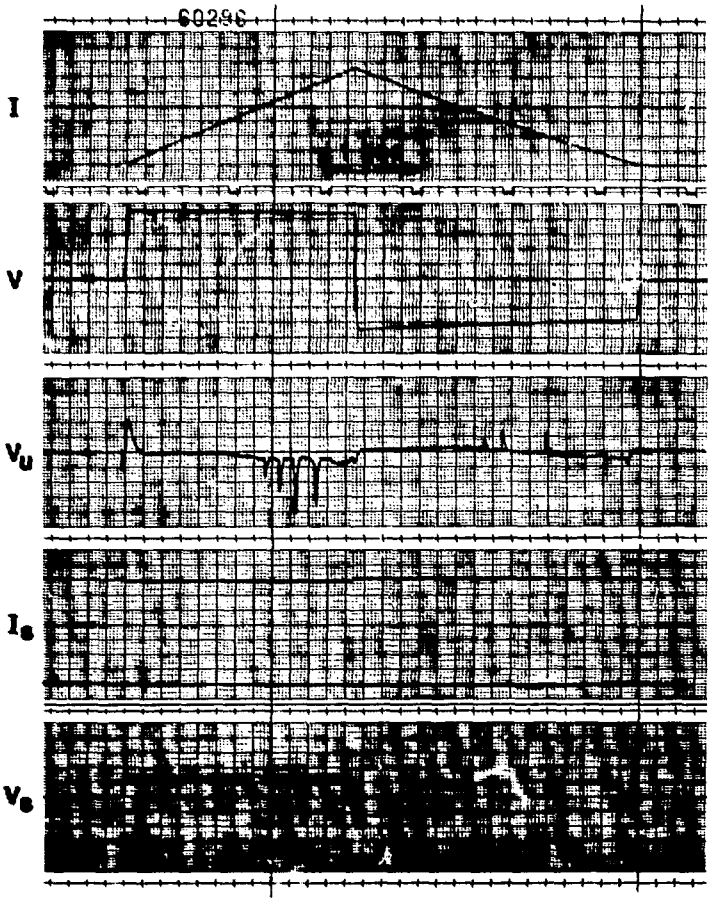

Fig. 4. Typical pulsing mode of the coil with a testing sample coil between the gap. I, pulsing current (20 A/div.); V, coil terminal voltage (2 V/div.); V_u, unbalanced voltage (0.4 m V/div.); I_s, transport current in the sample coil (10 A/div.); V_s, terminal voltage of the sample coil (1 m V/div.).

pulsing periods of 8 to 10 s. The recordings of the transport current, I_s, and voltage, V_s, of the non-perfect bipolar winding of the sample coil monitor whether the sample coil is quenched or not. The magnetic fields on the sample coil at the pulsing current of 640 A were in the range of 4.0 ~ 2.8 T.

The data of the loss measurements for the sample coils is shown in Fig. 5. Each data point of the ac losses in Fig. 5 is averaged over 30 to 50 pulses. The changes of the liquid helium level in the G-10 cylinder during the measurements of the average losses were typically 5 to 10 cm. The data in Fig. 5 shows that the ac losses of the cable with Formvar coated strands and

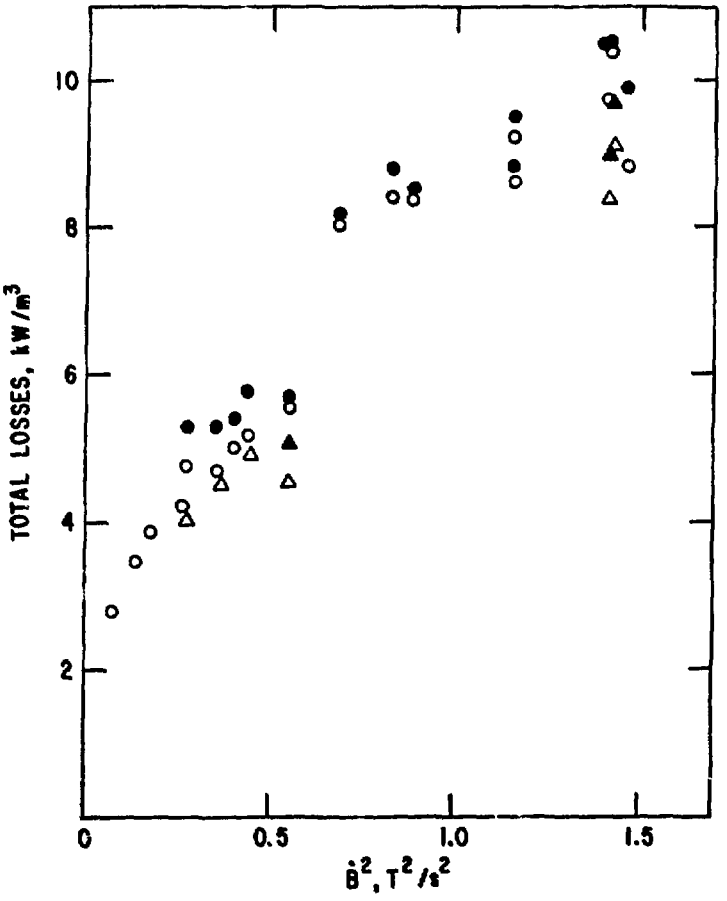

Fig. 5. Total ac losses per unit volume of the conductor vs. $\dot{B}^2$. (Data of triangles are from the triplex cable with Formvar-coated strands; those of circles are from the cable without Formvar-coated, open circles and triangles are without transport current; and closed circles and triangles are with a transport current of 350 A.

effective ramping time, t_e, is determined from the expression[2]

$$2/t_e = 1/t_u + 1/t_d \ , \tag{1}$$

those of the cable without the Formvar coating on the strands are virtually the same. This means that the data does not show any significant additional coupling losses among the bare superconducting strands. This may be due to the fact that the copper-nickel outer sheath has a quite high contact resistance among the strands. Also, the transport current of 350 A in the sample coil, which is less than 30% of the critical current, does not effect the ac losses significantly.

Figure 6 shows the data of the total ac losses per pulse. Assuming the current variations of the charge and discharge in Fig. 4 are linear, the where t_u and t_d are charging and discharging times, respectively. The maximum magnetic field B_m at the peak current is an averaged value over the sample coil. In order to determine the time constant, τ_o, from the expression for the coupling and eddy current losses, W_p, in the case of $t_e \gg \tau_o$,[3]

$$W_p = (B_m^2/2\mu_o)(R_f/R)^2(4\tau_o/t_e) \ , \tag{2}$$

the hysteresis losses of the sample coils were subtracted from the data of Fig. 6, and plotted in Fig. 7. In Eq. (2), R_f is the radius of the filament region of the strand and R is the radius of the strand.

The ratio of R_f/R is taken to be unity assuming the thickness of the outer sheath is small compared to the radius of the strand. From Fig. 7 and Eq. (2), τ_o is found to be approximately 3.8 to 5.7 ms. From the expression for the magnetic diffusion time constant,

$$\tau_o = (\mu_o/\rho_e)(\ell_p/2\pi)^2 \ , \tag{3}$$

and using the filament twist pitch length ℓ_p of 1.0 cm, the effective coupling resistivity of the strand, ρ_e, is found to be (5.0 to 7.5) $\times 10^{-10}$ Ω-m. This result is comparable to the previous measurements of a 0.51-mm strand (τ_o = 10 ms, $\rho_e = 5.1 \times 10^{-10}$ Ω-m).[4]

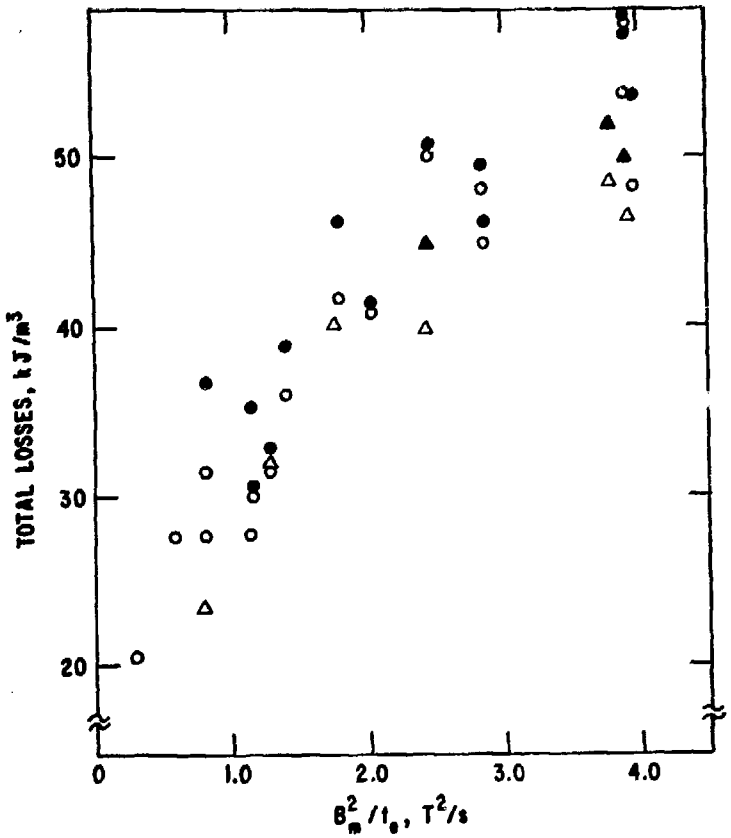

Fig. 6. Total ac losses per pulse per unit volume of the conductor vs. B_m^2/t_e. Data of triangles are from the triplex cable with Formvar-coated strands; those of circles are from the cable with Formvar coated; open circles and triangles are without transport current; and closed circles and triangles are with a transport current of 350 A.

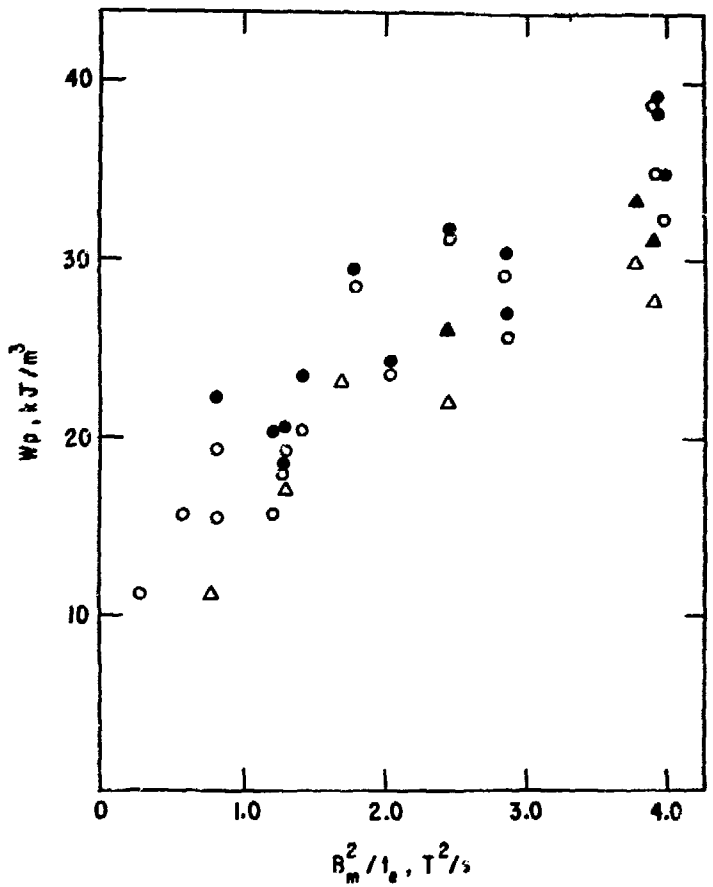

Fig. 7. Coupling and eddy current losses vs. B_m^2/t_e. Data of triangles are from the triplex cable with Formvar-coated strands; those of circles are from cable without Formvar coated; and open circles and triangles are with a transport current of 350 A.

In subtracting the hysteresis losses from the data of Fig. 6, the following expression for the hysteresis loss, Q/V_{sc} ($J \cdot m^{-3}$ pulse),

$$Q/V_{sc} = (4/3\pi)J_o B_o \, d \, \ln\{(B_m + B_o)/B_o\} , \qquad (4)$$

is used. Here V_{sc} is the volume of the superconducting filament only, d is the diameter of the filament, and $J_o = 9 \times 10^9$ A/m^2 and $B_o = 1$ T are constants for the expression of the critical current of NbTi filaments.

4. CONCLUSIONS

AC losses of two triplex cables were measured, one with Formvar coating on the superconducting strands and another without the coating. The results indicate that, because of the high resistance of the CuNi outer sheath of the superconducting strand, coupling among the bare strands seems to be very weak. In the regime of $\dot{B} = 0 \sim 1.2$ T/s and $B = 0 \sim 4$ T, the magnetic diffusion time constant τ_o was $(3.8\text{-}5.7) \times 10^{-3}$ s. The time constant could be reduced easily to a factor of one-fourth by reducing the twist pitch length ℓ_p by one half. Since practical conductors may be compacted to a certain degree during the cabling procedure, it may be necessary to measure the coupling losses when the subcables are compacted to $5 \sim 10\%$ in diameter.

ACKNOWLEDGMENTS

This work was supported by the Plasma Fusion Center of Massachusetts Institute of Technology. The author would like to thank D. B. Montgomery of MIT for helpful discussions, and W. Sampson of Brookhaven National Laboratory for supplying the superconducting wire.

REFERENCES

1. S. H. Kim, C. I. Krieger, and D. G. McGhee, "Further Tests of the Argonne 3.3 MJ Pulsed Superconducting Coil and its Nonmetallic Cryostat," IEEE Trans. on Magnetics MAG-19, 346 (1983).

2. H. Tateishi, T. Onishi, K. Komuro, and K. Koyama, "The Influence of Solder-filling on the AC Losses of Pulsed Superconducting Cables," Cryogenics 20, 509 (1982).

3. B. Turck, "Coupling Losses in Various Outer Normal Layers Surrounding the Filament Bundle of a Superconducting Composite," J. Appl. Phys. 50, 5397 (1979).

4. S. H. Kim, J. W. Dawson, D. G. McGhee, and S. S. Shen," AC Losses of 19-Strand Subcables for the ANL 3.3 MJ Coil," Adv. Cryogenic Engr. 30, 939 (1984).

Distribution for ANL/FPP/TM-200

Internal:

C. Baker
M. Billone
J. Brooks
Y. Cha
D. Ehst
K. Evans
P. Finn
Y. Gohar
D. Gruen
A. Hassanein
C. Johnson
J. Jung
S. Kim (3)
R. Kustom
R. Leonard
B. Loomis
S. Majumdar
R. Mattas
B. Misra
B. Picologlou
W. Praeg
D. Smith
H. Stevens
D-K. Sze
L. Turner
ANL Patent Dept.
FP Program (10)
ANL Contract File
ANL Libraries (2)
TIS Files (6)

External:

DOE-TIC, for distribution per UC-20, 20b, 20d (155)
Manager, Chicago Operations Office, DOE
Special Committee for Fusion Program:
- S. Baron, Brookhaven National Laboratory
- H. Forsen, Bechtel National, Inc., San Francisco
- J. Maniscalco, TRW, Inc., Redondo Beach
- G. Miley, University of Illinois-Urbana
- P. Reardon, Brookhaven National Laboratory
- P. Rutherford, Princeton Plasma Physics Laboratory
- D. Steiner, Rensselaer Polytechnic Institute
- K. Symon, Synchrotron Radiation Center, Stoughton, Wis.
- K. Thommassen, Lawrence Livermore National Laboratory

R. Boom, University of Wisconsin-Madison
E. Dalder, Lawrence Livermore National Laboratory
C. Henning, Lawrence Livermore National Laboratory
M. Lubell, Oak Ridge National Laboratory
D. Montgomery, Massachusetts Institute of Technology (3)
J. Purcell, GA Technologies
J. Rogers, Los Alamos National Laboratory
J. Schultz, Massachusetts Institute of Technology
G. Sheffield, Princeton Plasma Physics Laboratory
S. Shen, Oak Ridge National Laboratory